DALTON
FULL PAPER

Proton affinity of $[Fe_4S_4\{SCH_2CH(OH)Me\}_4]^{2-}$ in methanol: relevance to hydrogen bonding of Fe–S clusters in proteins †

Sian C. Davies,[a] David J. Evans,[a] Richard A. Henderson,*[b] David L. Hughes[a] and Steven Longhurst[a]

[a] *Department of Biological Chemistry, John Innes Centre, Norwich Research Park, Colney, Norwich, UK NR4 7UH*
[b] *Department of Chemistry, Bedson Building, University of Newcastle, Newcastle-upon-Tyne, UK NE1 7RU*

Received 8th June 2001, Accepted 12th October 2001
First published as an Advance Article on the web 14th November 2001

The reaction between PhS^- and $[Fe_4S_4\{SCH_2CH(OH)Me\}_4]^{2-}$ to form $[Fe_4S_4(SPh)_4]^{2-}$ has been studied in methanol, in the presence of the weak acid, $[NHEt_3]^+$. The kinetics are similar to those observed earlier for a variety of Fe–S-based clusters studied in MeCN. A major difference between the studies in the two solvents concerns the identity of the solution species. In MeCN, $[NHEt_3]^+$ is a sufficiently strong acid to convert all PhS^- to PhSH. However, in MeOH, PhSH is a comparatively stronger acid and consequently PhS^- is little protonated by $[NHEt_3]^+$. The rate law for the reaction in MeOH is consistent with a mechanism in which initial protonation of a thiolate ligand is followed by protonation of the cluster core (presumably a μ_3-S) which labilises the terminal thiol ligand. Subsequent attack of PhS^- at the vacant site thus created on one of the Fe atoms completes the first act of substitution. Analysis of the data yields $pK_a = 8.5$ for $[Fe_4S_3(\mu\text{-}SH)\{SCH_2CH(OH)Me\}_4]^-$. The relevance of this result to hydrogen bonding interactions of Fe–S-based clusters in proteins is discussed. The X-ray crystal structure of $[NMe_4]_2[Fe_4S_4\{SCH_2CH(OH)Me\}_4]$ is also reported, and the arrangement of the ligands is consistent with an extensive hydrogen bonding network between some of the hydroxyl groups.

Introduction

Fe–S-based clusters play a variety of roles in biology.[1,2] In addition to the ability to transfer and store electrons, Fe–S clusters can, in certain enzymes, be the site where the substrate is bound and transformed into products.

Protonation of synthetic Fe–S clusters has been known for several years. Thus, the substitution reactions of synthetic Fe–S-based clusters are accelerated in the presence of acid.[3,4] Indeed, for $[Fe_4S_4(SR)_4]^{2-}$ (R = alkyl), substitution does not occur in the absence of acid. In contrast, evidence for complete proton transfer to Fe–S clusters in proteins is scant. The only evidence for protonation of an Fe–S cluster in a protein, of which we are aware, is in ferredoxin I (Fe_3S_4 cluster) from *Azotobacter vinelandii* where the redox potential is pH dependent.[5]

The active sites in hydrogenases[6] and nitrogenases[7] comprise more elaborate Fe–S-based clusters, at which substrates bind, and are transformed *via* sequences of protonation (and electron transfer) reactions. Clearly, in hydrogenases and nitrogenases the active sites must operate in a protic environment. Theoretical calculations on the NiFe and Fe-only active sites of hydrogenase[8,9] indicate protonation of the sulfur ligands. Similarly, both theoretical studies[10] and kinetic studies on extracted FeMo-cofactor[11] from nitrogenase indicate protonation of μ_2-S or μ_3-S sites.

In proteins, complete proton transfer is perhaps unfavourable but can be replaced by partial proton transfer. Hydrogen bonding of cysteinate and μ_n-S ligands[12] of Fe–S-based clusters is widespread. In particular, the X-ray crystal structures of all proteins containing Fe–S clusters feature hydrogen bonding of main chain amide N–H to cluster sulfur atoms. However, amino acid side chains are also involved in hydrogen bonding in some systems. It seems reasonable to assume that the pK_a of the side chain will control the extent of proton transfer to the cluster. Since the substitution lability of synthetic Fe–S-based clusters is affected by protonation, it seems likely that the choice of hydrogen bond donor is a means of tuning the reactivity of the cluster. One of our goals is to develop a conceptual understanding of how the reactivity of Fe–S-based clusters is modulated by hydrogen bonds inside proteins. In this paper we report the determination of the pK_a associated with protonation of the cluster core in a protic solvent and discuss the relevance of our findings to hydrogen bonding in naturally-occurring Fe–S-based clusters.

Experimental

All manipulations in both the synthetic and kinetic aspects of this work were routinely performed under an atmosphere of dinitrogen using Schlenk and syringe techniques as appropriate. The compounds $[NHEt_3]Cl$,[13] and $[NEt_4]SPh$[14] were prepared by the literature methods.

All solvents were dried over the appropriate drying agent and distilled immediately prior to use: MeCN (CaH_2); tetrahydrofuran (sodium–benzophenone) and MeOH (NaOMe).

Mössbauer spectra were recorded at 77 K on an ES-Technology MS-105 spectrometer with a 925 MBq ^{57}Co source in a rhodium matrix at ambient temperature; NMR spectra on a Jeol Lambda 400 spectrometer and UV-visible absorption spectra on a Shimadzu UV-2101PC spectrophotometer.

Synthesis of $[NMe_4]_2[Fe_4S_4\{SCH_2CH(OH)Me\}_4]$

To a solution of $[NMe_4]_2[Fe_4S_4(SBu^t)_4]$[15] (0.43 g, 0.50 mmol) in acetonitrile (50 cm^3) were added 5 equivalents of 1-mercapto-

† Electronic supplementary information (ESI) available: kinetic data for the reaction of $[Fe_4S_4\{SCH_2CH(OH)Me\}_4]^{2-}$ with PhS^- in the presence of $[NHEt_3]^+$ in MeOH at 25 °C. See http://www.rsc.org/suppdata/dt/b1/b105075n/

 DOI: 10.1039/b105075n

2-propanol (0.23 g, 2.50 mmol). The solution was stirred for 30 minutes after which all volatiles were removed *in vacuo*. The residue was redissolved in warm acetonitrile (40 cm^3) and filtered. To the filtrate was added ethyl acetate (50 cm^3), dropwise. After storage at −18 °C overnight, the black crystalline product was collected by filtration, washed with ethyl acetate and dried *in vacuo* (60% yield).

Kinetic studies

The kinetics of the reaction between $[Fe_4S_4\{SCH_2CH(OH)Me\}_4]^{2-}$ ($[Fe_4S_4]$ = 0.1 mmol dm^{-3}) and PhS^-, in the presence of $[NHEt_3]^+$, were studied in MeOH using a Hi-Tech SF51 stopped-flow spectrophotometer, modified to handle air-sensitive solutions,[16] and interfaced to a Viglen computer *via* an analogue-to-digital converter. The temperature was maintained at 25.0 °C using a Grant LE8 thermostat tank.

Solutions containing mixtures of $[NHEt_3]Cl$ and $[NEt_4]SPh$ were prepared in dry MeOH from stock solutions of the reagents and used within 1 hour of preparation.

The kinetics of the reactions of $[Fe_4S_4\{SCH_2CH(OH)Me\}_4]^{2-}$ were studied by monitoring the absorbance change at λ = 520 nm. The absorbance–time traces were a good fit to two exponentials of equal magnitude, with the initial absorbance corresponding to that of $[Fe_4S_4\{SCH_2CH(OH)Me\}_4]^{2-}$ and the final absorbance to that of $[Fe_4S_4(SPh)_4]^{2-}$. Although $[NR_4]_2[Fe_4S_4(SPh)_4]$ is insoluble in methanol, its rate of precipitation in the reactions described herein was sufficiently slow that the substitution reaction could be studied before the solutions became heterogeneous.

The absorbance–time traces were fitted using a computer program, and the values of the observed rate constants (k_{obs}) were obtained from this analysis. The dependence of the reaction rates on the concentrations of PhS^- and $[NHEt_3]^+$ was established by the usual graphical methods [17] as described later.

Crystal structure analysis of $[NMe_4]_2[Fe_4S_4\{SCH_2CH(OH)Me\}_4]$

Crystal data: $2(C_4H_{12}N)$, $C_{12}H_{28}Fe_4O_4S_8$, M = 864.5. Monoclinic, space group $P2_1/a$ (equiv. to no. 14), a = 19.004(4), b = 10.715(4), c = 19.586(8) Å, β = 101.37(3)°, V = 3910(2) $Å^3$. Z = 4, D_c = 1.469 g cm^{-3}, $F(000)$ = 1800, T = 293 K, μ(Mo-Kα) = 19.1 cm^{-1}, λ(Mo-Kα) = 0.71069 Å.

Crystals are air-sensitive, very thin, black plates. One, *ca.* 0.02 × 0.55 × 0.57 mm, was mounted, under dinitrogen, on a glass fibre and coated with epoxy resin. After preliminary photographic examination (showing a poorly diffracting crystal), this was transferred to an Enraf-Nonius CAD4 diffractometer (with monochromated radiation) for determination of accurate cell parameters (from the settings of 25 reflections, θ = 8–10°, each centred in four orientations) and for measurement of diffraction intensities [3641 unique reflections to θ_{max} = 20°, the limit of useful measurement; 1670 were 'observed' with $I > 2\sigma_I$].

During processing, corrections were applied for Lorentz-polarisation effects, absorption (by semi-empirical Ψ-scan methods) and to eliminate negative net intensities (by Bayesian statistical methods). A small correction for crystal deterioration was also applied. The structure was determined by the direct methods routines in the SHELXS program [18] and refined by full-matrix least-squares methods, on F^2, in SHELXL.[19] Disorder in two of the thiolate ligands and one of the cations was identified. Hydrogen atoms were included in idealised positions in the fully ordered groups; no hydroxyl hydrogen atoms were located or estimated. The non-hydrogen atoms (except those which are disordered) were refined with anisotropic thermal parameters, and the H-atom U_{iso} values were set to ride on the U_{eq} values of the parent carbon atoms. The low resolution and low number of observed reflections limit the accuracy of the geometric parameters derived. At the conclusion of the refinement, wR_2 = 0.271 and R_1 = 0.151 [19] for all 3641 reflections weighted $w = [\sigma^2(F_o^2) + (0.1602P)^2]^{-1}$ with $P = (F_o^2 + 2F_c^2)/3$; for the 'observed' data only, R_1 = 0.090. In the final difference map, the highest peaks (to *ca.* 0.6 e $Å^{-3}$) were around the $\{Fe_4S_4\}$ core.

Scattering factors for neutral atoms were taken from reference 20. Computer programs used in this analysis have been noted above or in Table 4 of reference 21, and were run on a DEC-AlphaStation 200 4/100 in the Biological Chemistry Department, John Innes Centre.

CCDC reference number 168689.

See http://www.rsc.org/suppdata/dt/b1/b105075n/ for crystallographic data in CIF or other electronic format.

Results and discussion

We have been studying the kinetics of the substitution reactions of synthetic Fe–S-based clusters in the presence of weak acids such as $[NHEt_3]^+$, $[lutH]^+$ (lut = 2,6-dimethylpyridine) and $[\overline{NH_2(CH_2)_3CH_2}]^+$ which allows us to get information about protonation of these clusters. The approach we have developed makes use of the observation that the rate of substitution of the terminal ligands is sensitive to the state of protonation of the cluster. The mechanism we have proposed is summarised in Fig. 1.

The following entirely general characteristics have emerged from our studies in MeCN. (1) The act of substitution is rate-limiting when protonation is thermodynamically favourable.[22,23] (2) Clusters with terminal thiolate ligands undergo substitution by dissociative mechanisms whilst clusters with halido-ligands undergo substitution by associative mechanisms.[24] (3) $[NHEt_3]^+$ (pK_a = 18.46 in MeCN) only singly protonates Fe–S-based clusters.[22–25] (4) $[lutH]^+$ (pK_a = 15.4) can doubly protonate clusters.[26] (5) With $[\overline{NH_2(CH_2)_3CH_2}]^+$ (pK_a = 21.5) protonation is thermodynamically unfavourable and thus protonation becomes rate-limiting.[27] (6) Sequential addition of two protons to the cluster core progressively labilises thiolate clusters towards substitution, but for the chloro-analogues addition of the first proton labilises whilst addition of the second inhibits substitution.[26] (7) The pK_a of the singly protonated cluster is insensitive to the structure of the cluster, the overall charge, the composition of the cluster core and the identity of the terminal ligands. The value falls in the narrow range $pK_a = 18.4 \pm 0.5$ for all synthetic clusters so-far studied.[28] (8) The pK_a of the second protonation depends on the terminal ligands (*ca.* 16.5 for chloro-clusters and *ca.* 13.5 for thiolato-clusters). This is not because protonation occurs at the terminal ligand. Rather it is a consequence of the electronic response of the terminal ligand to the addition of the first protonation.[26]

Whilst we have previously reported extensive studies on a variety of structurally diverse Fe–S-based clusters, ranging from $[Fe_2S_2Cl_4]^{2-}$ to FeMo-cofactor extracted from the enzyme nitrogenase,[29,30] this is the first time we have investigated the influence that the solvent has on these reactions. Studies in a protic solvent are crucial in order to discuss confidently the physiological relevance of protonation of Fe–S clusters in proteins.

Synthesis and characterisation of $[NMe_4]_2[Fe_4S_4\{SCH_2CH(OH)Me\}_4]$

$[NMe_4]_2[Fe_4S_4\{SCH_2CH(OH)Me\}_4]$ was prepared by the metathetical reaction shown in eqn. (1), and was obtained in *ca.* 60% yield. The reaction is facilitated by the removal of the volatile Bu^tSH. The black crystalline product was characterised by elemental analysis, ^1H and ^{13}C NMR, UV-visible and Mössbauer spectroscopies, as shown in Table 1 and the X-ray crystallography data. The spectroscopic parameters were as expected for a mercaptoalcohol-ligated Fe_4S_4 cluster.[31]

The stability of the cluster in water was examined by measuring the UV-visible spectrum over extended periods. The cluster

Table 1 Elemental analysis and spectroscopic characterisation of $[NMe_4]_2[Fe_4S_4\{SCH_2CH(OH)Me\}_4]$

Elemental Analysis[a] (%)	C	H	N
	28.0	6.1	3.2
	(27.8)	(6.1)	(3.2)
Mossbauer Parameters[b]	isomer shift/mm s^{-1}	quadrupole splitting/mm s^{-1}	
	0.43	1.22	
Electronic Spectrum[c]	λ_{max}/nm	ε/dm^3 mol^{-1} cm^{-1}	
	296	22,340	
	373	8,690	
	416	4,720	
^{1}H NMR Spectrum[c]	δ/ppm	assignment	
	12.9 and 12.2	SCH_2	
	4.2	O*H*	
	3.7	C*H*OH	
	3.1	$[NMe_4]^+$	
	1.6	CH_3	
^{13}C NMR Spectrum[c]	δ/ppm	assignment	
	101	*C*-S	
	65	*C*-OH	
	56	$[NMe_4]^+$	
	22	CH_3	

[a] Calculated values shown in parentheses. [b] Solid state spectrum. Errors ≤ ±0.01 mm s^{-1}, half width at half maxima = 0.15 mm s^{-1}. Referenced to natural Fe at 298 K. [c] Solvent = dmso.

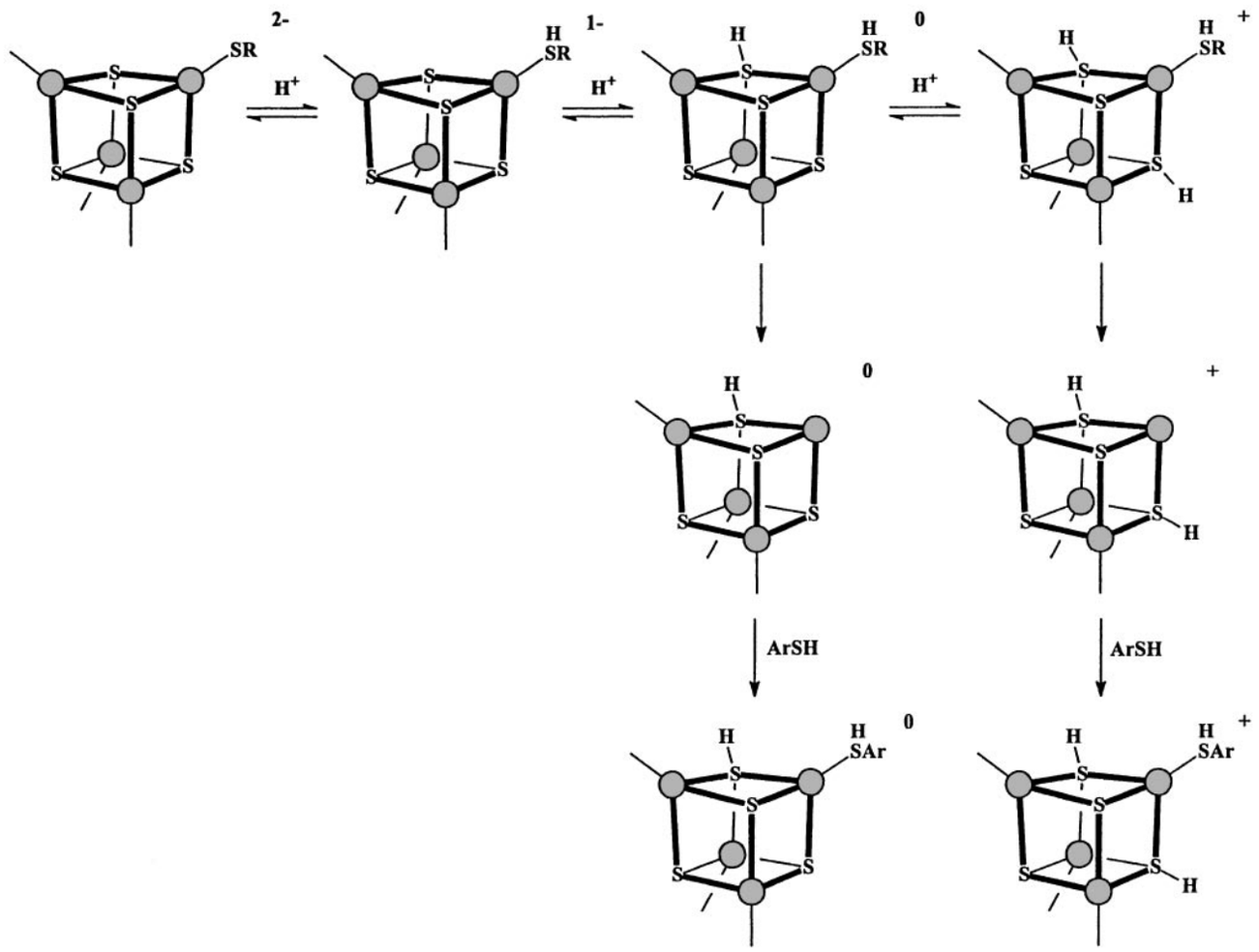

Fig. 1 General mechanism for the acid-catalysed substitution reactions of synthetic Fe–S-based clusters.

$$[Fe_4S_4(SBu^t)_4]^{2-} + 4MeCH(OH)CH_2SH \longrightarrow [Fe_4S_4\{SCH_2CH(OH)Me\}_4]^{2-} + 4Bu^tSH \quad (1)$$

is stable for at least 2 h, with no significant change in the spectrum. After 24 h a small spectral change is evident, probably due to partial hydrolysis. The stopped-flow experiments were performed in MeOH and completed within 1 h to ensure that the cluster is not subject to appreciable decomposition.

Description of the crystal structure of $[NMe_4]_2[Fe_4S_4\{SCH_2CH(OH)Me\}_4]$

The structure of the cluster anion is illustrated in Fig. 2, with principal bond lengths and angles shown in Table 2. The crystals were obtained directly from the preparation. No further recrystallization was required.

The Fe_4S_4 core is well defined and structurally similar to other reported like structures. There is no precise crystallographic symmetry within the ion, but the core does show

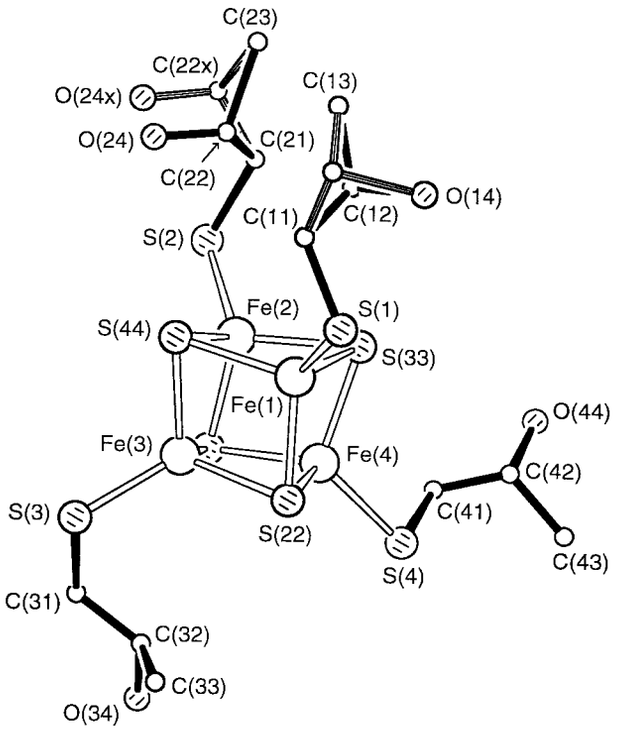

Fig. 2 View of the anion in $[NMe_4]_2[Fe_4S_4\{SCH_2CH(OH)Me\}_4]$.

pseudo $-42m$ symmetry. The ligand arrangement, although not unique, is somewhat unusual in that three thiolate ligands are roughly parallel to a pseudo -4 axis whilst the fourth, of S(4), lies approximately normal to that axis. There is disorder in the two upper ligands in Fig. 2, with that of S(1) showing alternative sites for the β-C atom, and that of S(2) alternative sites for the β-C and the oxygen atoms. Each of the four ligands contains a chiral centre. The disorder allows thiolate ligands of either chirality to be bound at the Fe(1) and Fe(2) sites; the remaining two ligands were well resolved, that of S(3) with an *S*-configuration, and that of S(4) with an *R*-configuration. The crystal has a centrosymmetric space group and therefore contains anions also of the inverted structure.

The arrangement of ligands might be a consequence of the hydrogen bonding network. We propose that there are hydrogen bonds between O(34) and O(44′) and, by symmetry, between O(44) and O(34′), thus forming a hydrogen-bonded dimer of two anions about a centre of symmetry. There is further bonding between O(34) and O(44″), O(44) and O(34‴), *etc.*, which links the dimer units in chains as shown in Fig. 3. We note here the formation of a cyclic arrangement of four hydrogen-bonded hydroxyl groups around a centre of symmetry; the direction of the bonding is not clear since the hydrogen atoms have not been located, but the C–O ⋯ O angles (Table 2) suggest that the bonds might go in either direction. The disordered ligands are not involved in hydrogen bonds and are linked to neighbouring ions only through normal van der Waals' interactions.

One of the $[NMe_4]^+$ cations is well resolved and has a good tetrahedral arrangement of methyl groups. However, the other cation shows signs of disorder with at least two orientations with an occupation ratio of *ca.* 55 : 45. Resolution of the refined sites into two distinct atom sites was not feasible in some cases. The cations are arranged so that the methyl groups lie flat against the Fe_2S_2 faces of the $\{Fe_4S_4\}$ cube and lie between the sheets of the anions.

Reaction between $[Fe_4S_4\{SCH_2CH(OH)Me\}_4]^{2-}$ and PhS^- in MeOH

The reaction between $[Fe_4S_4\{SCH_2CH(OH)Me\}_4]^{2-}$ and PhS^- ultimately produces $[Fe_4S_4(SPh)_4]^{2-}$ as shown in eqn. (2).

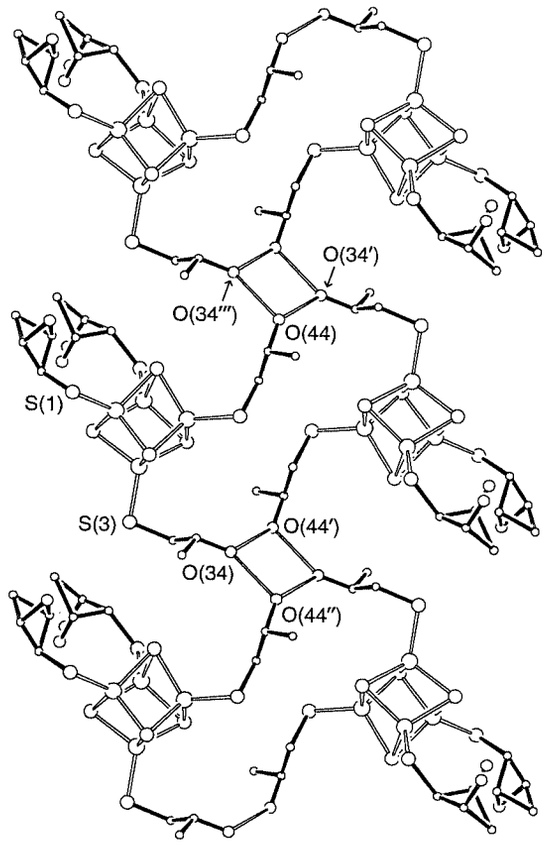

Fig. 3 The hydrogen bonding network within a crystal of $[NMe_4]_2[Fe_4S_4\{SCH_2CH(OH)Me\}_4]$.

$$[Fe_4S_4\{SCH_2CH(OH)Me\}_4]^{2-} + 4PhS^- \longrightarrow [Fe_4S_4(SPh)_4]^{2-} + 4MeCH(OH)CHCH_2SH \quad (2)$$

Ideally we wanted to study the reaction between $[Fe_4S_4\{SCH_2CH(OH)Me\}_4]^{2-}$ and PhS^- in water, however this proved impractical for two reasons. Firstly, $[NEt_4]SPh$ is very insoluble in water. Although NaSPh could be used as an alternative source of PhS^-, previous work has shown that Na^+ ions can bind to Fe–S clusters and affect the kinetics.[32] Secondly, the product of the reaction, $[Fe_4S_4(SPh)_4]^{2-}$, is very insoluble in water. However, $[NEt_4]SPh$ is soluble in MeOH and furthermore $[NR_4]_2[Fe_4S_4(SPh)_4]$ precipitates relatively slowly from this solvent under the experimental conditions employed. Thus, kinetic data for the substitution reaction can be collected before the solutions become turbid.

When studied using a stopped-flow apparatus, the reaction between $[Fe_4S_4\{SCH_2CH(OH)Me\}_4]^{2-}$ and PhS^- in the presence of $[NHEt_3]^+$ is typified by an absorbance–time trace that can be fitted to two exponentials. As in earlier studies, we are concerned primarily with the first act of substitution and hence the following discussion will concentrate only on the faster process.

The exponential shape of the absorbance–time curves indicates that the reaction exhibits a first order dependence on the concentration of the cluster. This was confirmed by studies in which the concentration of the cluster was varied in the range $[Fe_4S_4\{SCH_2CH(OH)Me\}_4^{2-}] = 0.025$–$0.10$ mmol dm^{-3} whilst keeping the concentrations of PhS^- (2.0 mmol dm^{-3}) and $[NHEt_3]^+$ (10.0 mmol dm^{-3}) constant. Under these conditions the observed rate constant did not vary ($k_{obs} = 3.1 \pm 0.1$).

In order to analyse the dependence of the reaction rate on concentrations of PhS^-, $[NHEt_3]^+$ and NEt_3 it is important to consider the protolytic equilibrium shown in eqn. (3).

$$PhS^- + [NHEt_3]^+ \rightleftharpoons PhSH + NEt_3 \quad (3)$$

Table 2 Selected molecular dimensions (bond lengths are in Ångstroms, angles in degrees; e.s.d.s are in parentheses)

(a) In the Fe_4S_4 cluster			
Fe(1) ··· Fe(2)	2.717(3)	Fe(2) ··· Fe(3)	2.729(4)
Fe(1) ··· Fe(3)	2.720(4)	Fe(2) ··· Fe(4)	2.733(4)
Fe(1) ··· Fe(4)	2.737(4)	Fe(3) ··· Fe(4)	2.759(4)
Fe(1)–S(22)	2.244(6)	Fe(3)–S(11)	2.299(5)
Fe(1)–S(33)	2.301(6)	Fe(3)–S(22)	2.302(6)
Fe(1)–S(44)	2.288(6)	Fe(3)–S(44)	2.247(6)
Fe(2)–S(11)	2.260(6)	Fe(4)–S(11)	2.283(5)
Fe(2)–S(33)	2.286(6)	Fe(4)–S(22)	2.293(6)
Fe(2)–S(44)	2.296(6)	Fe(4)–S(33)	2.254(6)
S(22)–Fe(1)–S(33)	103.6(2)	S(11)–Fe(3)–S(22)	103.9(2)
S(22)–Fe(1)–S(44)	104.4(2)	S(11)–Fe(3)–S(44)	104.2(2)
S(22)–Fe(1)–S(1)	115.7(2)	S(11)–Fe(3)–S(3)	113.5(2)
S(33)–Fe(1)–S(44)	105.4(2)	S(22)–Fe(3)–S(44)	103.9(2)
S(33)–Fe(1)–S(1)	115.4(3)	S(22)–Fe(3)–S(3)	116.8(2)
S(44)–Fe(1)–S(1)	111.2(2)	S(44)–Fe(3)–S(3)	113.3(2)
S(11)–Fe(2)–S(33)	103.5(2)	S(11)–Fe(4)–S(22)	104.7(2)
S(11)–Fe(2)–S(44)	103.9(2)	S(11)–Fe(4)–S(33)	103.8(2)
S(11)–Fe(2)–S(2)	114.3(2)	S(11)–Fe(4)–S(4)	116.7(2)
S(33)–Fe(2)–S(44)	105.6(2)	S(22)–Fe(4)–S(33)	103.5(2)
S(33)–Fe(2)–S(2)	114.1(2)	S(22)–Fe(4)–S(4)	110.6(2)
S(44)–Fe(2)–S(2)	114.2(2)	S(33)–Fe(4)–S(4)	116.1(2)
Fe(2)–S(11)–Fe(3)	73.5(2)	Fe(1)–S(33)–Fe(2)	72.6(2)
Fe(2)–S(11)–Fe(4)	74.0(2)	Fe(1)–S(33)–Fe(4)	73.9(2)
Fe(3)–S(11)–Fe(4)	74.1(2)	Fe(2)–S(33)–Fe(4)	74.0(2)
Fe(1)–S(22)–Fe(3)	73.5(2)	Fe(1)–S(44)–Fe(2)	72.7(2)
Fe(1)–S(22)–Fe(4)	74.2(2)	Fe(1)–S(44)–Fe(3)	73.7(2)
Fe(3)–S(22)–Fe(4)	73.8(2)	Fe(2)–S(44)–Fe(3)	73.8(2)
(b) In the thiolate ligands			
Fe(1)–S(1)	2.243(7)	Fe(3)–S(3)	2.234(7)
Fe(2)–S(2)	2.237(7)	Fe(4)–S(4)	2.254(6)
Fe(1)–S(1)–C(11)	103.4(11)	Fe(3)–S(3)–C(31)	104.6(8)
Fe(2)–S(2)–C(21)	105.3(12)	Fe(4)–S(4)–C(41)	100.8(9)
(c) Proposed hydrogen bond connections			
O(34) ··· O(44′)	2.76(2)	O(34) ··· O(44″)	2.71(2)
C(32)–O(34) ··· O(44′)	123.6(13)	C(42)–O(44) ··· O(34′)	143.4(14)
C(32)–O(34) ··· O(44″)	138.4(13)	C(42)–O(44) ··· O(34‴)	123.9(14)

Primed atoms are of symmetry-related ions: $'\ -x, -y, -z$; $''\ x, y-1, z$; $'''\ x, y+1, z$.

Using $pK_a^{NH} = 10.7$[33] and $pK_a^{PhSH} = 6.6$,[34] the equilibrium constant for eqn. (3) in methanol can be calculated, $K = 8.0 \times 10^{-5}$. It is clear that the position of the equilibrium lies to the left-hand side, and the dominant nucleophile solution species is PhS^-. In contrast, in MeCN, the equilibrium constant for eqn. (3) is such that, in the presence of an excess of $[NHEt_3]^+$, all PhS^- is convert into PhSH. The reason for the marked difference in the equilibrium constants in MeCN and MeOH is because of the differential effect that these two solvents have on the pK_a's of PhSH and $[NHEt_3]^+$. Thus, in formally transferring from MeOH to MeCN, the pK_a of $[NHEt_3]^+$ changes from 10.7 to 18.4; $\Delta pK_a = 7.7$. In contrast the change in the pK_a of PhSH is $\Delta pK_a = 14.4$. The markedly different effects that MeCN and MeOH have on the acidities of $[NHEt_3]^+$ and PhSH are probably because ionisation of $[NHEt_3]^+$ produces a neutral conjugate base, whereas ionisation of PhSH produces an anionic conjugate base. Solvation of anions is poor in aprotic solvents like MeCN. Effects analogous to those described here have been noted before.[35] In particular, for ammonium ions, the formal transfer from water to MeCN is associated with $\Delta pK_a = 7.6 \pm 0.5$, whilst for a variety of substituted phenols $\Delta pK_a = 14.3 \pm 2.3$.

Using $K = 8.0 \times 10^{-5}$, the concentrations of PhS^-, PhSH, $[NHEt_3]^+$ and NEt_3 were calculated for all the conditions used experimentally. The rate of the reaction between $[Fe_4S_4\{SCH_2CH(OH)Me\}_4]^{2-}$ and PhS^- depends on the ratio $[NHEt_3^+]/[NEt_3]$ as shown in Fig. 4.

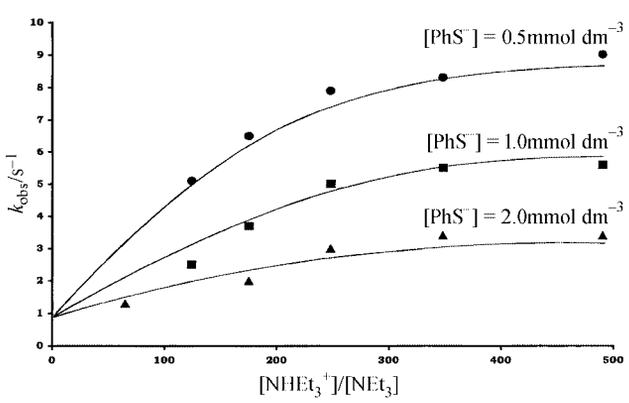

Fig. 4 Graph of k_{obs} against $[NHEt_3^+]/[NEt_3]$ for the reaction of PhS^- with $[Fe_4S_4\{SCH_2CH(OH)Me\}_4]^{2-}$ in MeOH at 25.0 °C. Data points correspond to: $[PhS^-] = 0.5$ mmol dm^{-3}, $[NHEt_3^+] = 0.63$–10.0 mmol dm^{-3} (●); $[PhS^-] = 1.0$ mmol dm^{-3}, $[NHEt_3^+] = 0.63$–25.0 mmol dm^{-3} (■); $[PhS^-] = 2.0$ mmol dm^{-3}, $[NHEt_3^+] = 2.5$–25.0 mmol dm^{-3} (▲). The ratio $[NHEt_3^+]/[NEt_3]$ was calculated using eqn. (3) and $K = 8.0 \times 10^{-5}$. The curves drawn are those defined by eqn. (4). All data were collected at $\lambda = 520$ nm.

The kinetics are complicated. In the absence of acid, substitution still occurs by a pathway which exhibits a first order dependence on the concentration of cluster but is independent

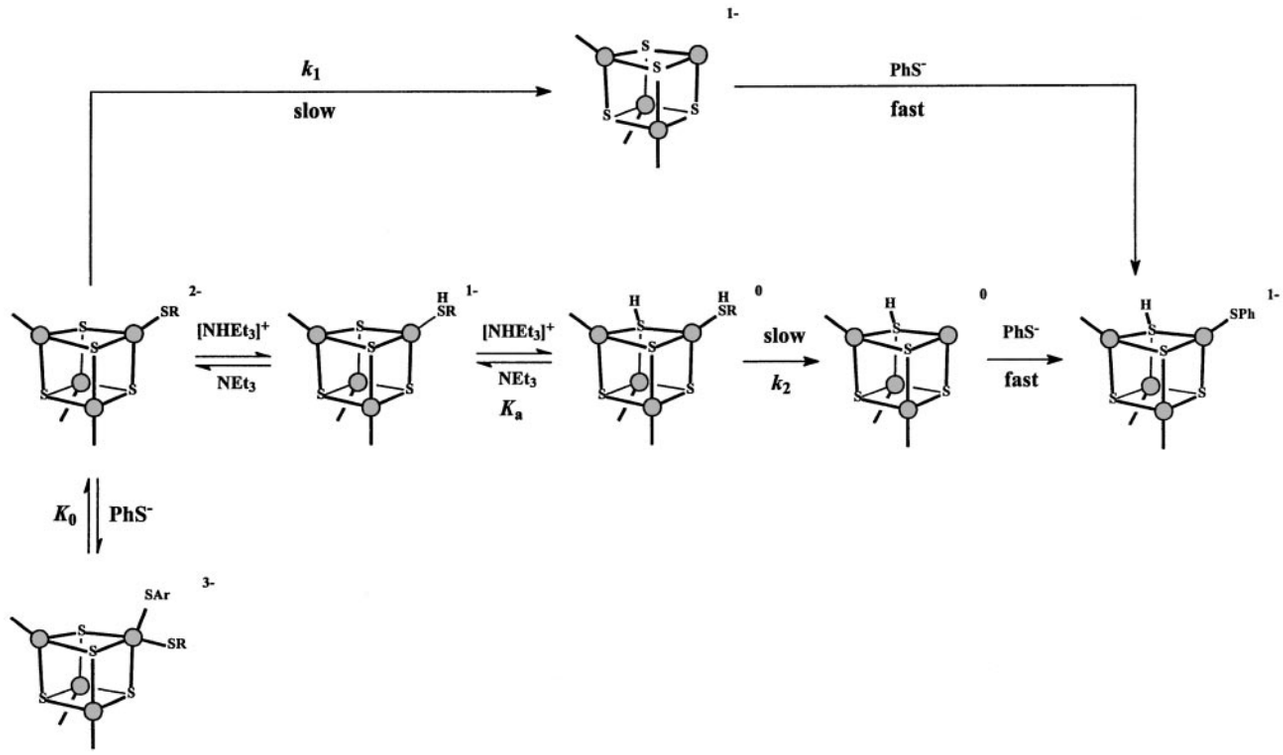

Fig. 5 Mechanism of the reaction between PhS^- and $[Fe_4S_4\{SCH_2CH(OH)Me\}_4]^{2-}$ in the presence of $[NHEt_3]^+$ in MeOH.

$$-\frac{d[Fe_4S_4\{SCH_2CH(OH)Me\}_4^{2-}]}{dt} = \frac{\{(1.0\pm0.2)+(0.14\pm0.02)([NHEt_3^+]/[NEt_3])\}[Fe_4S_4\{SCH_2CH(OH)Me\}_4^{2-}]}{1+(5.7\pm0.5)\times10^{-3}([NHEt_3^+]/[NEt_3])+(2.0\pm0.3)\times10^{3}[PhS^-]} \quad (4)$$

of the concentration of PhS^- (k_{obs} = 1.0 s^{-1}). At low values of $[NHEt_3^+]/[NEt_3]$, the rate of the reaction increases linearly with this ratio, but at high values of $[NHEt_3^+]/[NEt_3]$ the rate becomes independent of this ratio. One further feature is evident. In experiments where $[NHEt_3^+]/[NEt_3]$ is kept constant, the rate of the reaction is inhibited by increasing the concentration of PhS^-. The experimental rate law is shown in eqn. (4).

A similar rate law has been observed previously[23] in the reaction of $[Fe_4S_4(SR)_4]^{2-}$ (R = Et or Bu) with PhSH in MeCN. This indicates that the mechanisms for the reactions are analogous. The mechanism is shown in Fig. 5.

Earlier studies[22–30] on the acid-catalysed substitution reactions of Fe–S-based clusters in MeCN have indicated that the protonation of a μ_3-S is the major labilising force in this class of reactions. This pathway is shown in the centre of Fig. 5, and the rate-law associated with this pathway is shown in eqn. (5).

$$-\frac{d[Fe_4S_4\{SCH_2CH(OH)Me\}_4^{2-}]}{dt} = \frac{\{k_1+k_2K_a([NHEt_3^+]/[NEt_3])\}[Fe_4S_4\{SCH_2CH(OH)Me\}_4^{2-}]}{1+K_a([NHEt_3^+]/[NEt_3])} \quad (5)$$

Earlier studies have strongly indicated that protonation is at the cluster core. In particular, K_a is insensitive to: (i) the terminal ligand (alkyl thiolate, aryl thiolate or halide); (ii) the charge on the cluster; (iii) the cluster core structure and (iv) the metal composition of the cluster. Indeed, for *all* Fe–S-based clusters studied to date, pK_a = 18.4 ± 0.5 in MeCN.

We have argued before that it seems intuitively more reasonable that terminal thiolate ligands will be more basic than μ_3-S.[28] The reason protonation of thiolate ligands is not observed highlights a limitation of our approach. Protonation of the cluster is detected by monitoring the effect that protonation has on the rate of substitution. If protonation of a thiolate ligand does not affect the substitution lability of the cluster, then it is not possible to detect protonation by the kinetic approach described here.

Our studies here and elsewhere indicate that protonation of thiolate to a thiol has little effect on the lability. The thiolate ligand is a good σ-donor. Upon protonation, the corresponding thiol will be a poorer σ-donor but a better π-acceptor. Diminished σ-donation is compensated by π-backbonding, resulting in the bond strengths of thiolate and the corresponding thiol being similar, and hence labilities essentially the same. Compensatory bonding effects, such as these, have also been observed in structural studies on mononuclear Fe–thiolate systems.[36] In the reactions of the Fe–S-based clusters, further protonation of a μ_3-S adjacent to the coordinated thiol competes for the π-electron density, thus diminishing the π-backbonding to the thiol, weakening the Fe–thiol bond and labilising the cluster towards dissociation.

One additional kinetic feature has to be accommodated in the mechanism: the decrease in the rate of the reaction as the concentration of PhS^- is increased. Such behaviour has been observed in the reactions[23] of $[Fe_4S_4(Salkyl)_4]^{2-}$, but is not observed with the analogous $[Fe_4S_4(Salkyl)_4]^{2-}$. We attribute the inhibitory effect to the binding of PhS^- to $[Fe_4S_4(SR)_4]^{2-}$. However, the binding of PhS^- to the cluster does not lead to a facile pathway for substitution. Rather, the acid-catalysed route is the more rapid route.

The full rate law describing all the pathways illustrated in Fig. 5, is that shown in eqn. (6), which is readily derived by consider-

$$-\frac{d[Fe_4S_4]}{dt} = \frac{\{k_1+k_2K_a([NHEt_3^+]/[NEt_3])\}[Fe_4S_4\{SCH_2CH(OH)Me\}_4^{2-}]}{(1+K_a([NHEt_3^+]/[NEt_3])+K_o[PhSH])} \quad (6)$$

ing that K_a and K_o are equilibria, rapidly established prior to rate-limiting dissociation of the thiol ligand, k_2. Comparison of

eqn. (4) and (6) gives: $k_1 = 1.0 \pm 0.2\ s^{-1}$; $k_2 = 24.7 \pm 0.9\ s^{-1}$; $K_a = (5.7 \pm 0.5) \times 10^{-3}$ and $K_o = (2.0 \pm 0.3) \times 10^3\ dm^3\ mol^{-1}$.

The pK_a of $[Fe_4S_3(SH)\{SCH_2CH(OH)Me\}_4]^-$

Previous studies on the acid-catalysed substitution reactions of Fe–S-based clusters in MeCN have shown that the pK_a(MeCN) associated with the protonation of μ_n-S is 18.4 ± 0.5 for *all* synthetic Fe–S-based clusters studied to date. The wide-spread occurrence of Fe–S-based clusters in a variety of metalloenzymes raises the question whether protonation of the cluster core is a biologically significant reaction. It is possible to estimate the pK_a in MeOH using eqn. (7), which gives pK_a(MeOH) = 10.9 ± 0.5. However, this value is, at best, only approximate. Even a cursory look at the literature values for the pK_a's of a variety of acids in different solvents [35,37] shows that eqn. (7) is only valid for ammonium ions. As we have discussed above, the charges of the acid and corresponding conjugate base are important factors in defining the pK_a in different solvents. A particular concern in the present work is that we are trying to estimate the pK_a of a cluster where the acid is a monoanion and the conjugate base is a dianion.

$$pK_a(MeCN) - 7.5 = pK_a(MeOH) \qquad (7)$$

Using the data presented in this paper we can calculate the pK_a of $[Fe_4S_4\{SCH_2CH(OH)Me\}_4]^{2-}$ in MeOH. Since $K_a = K_a^{NH}/K_a^{cluster}$, and using $pK_a^{NH} = 10.7$ for $[NHEt_3]^+$, we can calculate $K_a^{cluster} = 3.5 \times 10^{-9}$ and hence $pK_a^{cluster} = 8.5$ in methanol. Previous work on $[Fe_4S_4(SCH_2CH_2CO_2)_4]^{6-}$ indicated that pK_a = 7.4 for protonation of the cluster core in water.[4] Since both water and methanol are protic solvents, the pK_a we have determined in MeOH seems reasonable.

For the first time we have shown that the mechanism of the acid-catalysed substitution reactions of synthetic Fe–S clusters is the same in MeOH as it is in MeCN, and that protonation of μ_3-S in $[Fe_4S_4\{SCH_2CH(OH)Me\}_4]^{2-}$ in the protc solvent is associated with a pK_a which is physiologically significant. We are now in a position to discuss the relevance of this result to Fe–S clusters in proteins.

Protonation and hydrogen bonding in naturally-occurring Fe–S clusters

In this section some general features concerning hydrogen bonding of Fe–S-based clusters in proteins will be considered, and how this possibly affects their reactivity. It is most revealing to consider electron transfer proteins separately from enzymes where the cluster is the substrate binding site.

The results presented above show that in a protic environment the pK_a of the protonated cluster is 8.5. In addition, our earlier extensive studies in MeCN indicate that this pK_a is common for all Fe–S-based clusters. Together, these two observations indicate that in proteins any amino acid side chain with p$K_a \leq 7.5$ will protonate Fe–S-based clusters. Thus, aspartic acid (pK_a = 3.7), glutamic acid (4.25), and protonated histidine (6.0) are all capable of protonating the cluster core. Although weaker acids such as tyrosine (pK_a = 10.1), lysine (10.8) and arginine (12.5) cannot transfer a proton to the cluster, they can still hydrogen bond to the cluster and hence modulate its reactivity. It seems reasonable that the extent of proton transfer within the hydrogen bond is proportional to $\Delta pK_a = pK_a^{H\text{-}donor} - 8.5$. Indeed, it has been proposed [38] that reactions affected by protonation (such as the substitution of the Fe–S-based clusters) will also be facilitated (but to a lesser extent) by partial proton transfer in hydrogen bonds.

The hydrogen bonding motifs of a variety of different Fe–S clusters have recently been reviewed.[12] $\{Fe_4S_4(Scysteinate)_4\}$ clusters in ferredoxins, from a variety of sources, all exhibit eight amide N–H hydrogen bonds to μ_3-S or cysteinate sulfur. In the iron–sulfur protein HiPIP, five such amide hydrogen bonds are evident. The high pK_a of amide N–H (*ca.* 17) means that these hydrogen bonds are best represented as N–H ⋯ S (*i.e.* little transfer of the proton to the cluster). Similar hydrogen bonds are evident in $\{Fe_2S_2\}$ and $\{Fe_3S_4\}$ clusters.

Interestingly, Fe–S-based clusters involved in substrate binding and transformation are hydrogen-bonded by other amino acid residues in addition to the amide groups. Thus, in the $\{Fe_4S_4\}$ cluster of aconitase (an enzyme that catalyses the equilibration of citrate and iso-citrate),[39] two aspartic amino acid residues hydrogen bond to μ_3-S or cysteinate sulfur. In this system the proton transfer to the cluster would appear to be complete (*i.e* O ⋯ H–S). Our work on synthetic Fe–S clusters indicates that such protonation labilises the cluster towards dissociation. It seems reasonable that protonation of the cluster in aconitase may be instrumental in facilitating the binding of the substrate at one of the Fe sites. It is worth emphasising that modulating the reactivity of a site during turnover may require hydrogen bonds to be made and broken in concert with the catalysis. The protein crystal structure data provide a "snap shot" of one particular state of the active site and do not reveal the potential dynamic aspects of hydrogen bonding.

The active site in the enzyme nitrogenase [40] (which catalyses the conversion of molecular nitrogen into ammonia) is FeMo-cofactor, a cluster of composition $MoFe_7S_9$ which is ligated to the polypeptide *via* a cysteinate to the unique tetrahedral Fe and a histidine to the six-coordinate Mo. FeMo-cofactor is hydrogen-bonded to the NH groups of Glyα356 and Glyα357, and also to Argα96, Argαs359 and Hisα195. These residues are all centred around the middle section of the cluster and it has been proposed [40] that the positive charges on these groups provide an electrostatic mechanism whereby negative charged intermediates are stabilised. This proposal is in line with our arguments but we can be a little more specific: it is the degree of proton transfer from these residues which is affecting the reactivity of the cofactor. Whilst Argα96 and Argα359 (pK_a = 12.5) can only be involved in partial proton transfer, complete proton transfer would occur from protonated Hisα195 (pK_a = 6) to the cluster.

The results of certain site-directed mutagenesis experiments can be rationalised in terms of hydrogen bonding effects. Intriguingly, mutation of Hisα195 for Gluα195 results in a nitrogenase which binds dinitrogen but does not convert it into ammonia,[41] whilst mutation of Hisα195 for Aspα195 (and a variety of other amino acids) produces an enzyme incapable of even binding dinitrogen. We would argue that these rather dramatic differences in reactivity are not so much a consequence of changing the amino acid as changing the state of protonation of the cluster. Both His and Glu can hydrogen bond to the cofactor but whereas with Hisα195 the cluster is protonated, with Gluα195 (pK_a = 17) it is not. In the case of the Aspα195 derivative the side chain is one CH_2 group shorter than Glu and so no hydrogen bond can be formed. Recently, theoretical studies have also proposed that the different reactivities of these nitrogenase mutants are due to the various hydrogen bonding capabilities of the amino acid side chains.[42]. However, the theoretical work proposes that the hydrogen bonds are to a dinitrogen molecule adsorbed on the cofactor. Our results on synthetic Fe–S clusters indicate that the cluster core is sufficiently basic to be protonated.

In this discussion we have concentrated on the effect of hydrogen bonding on the reactivities of Fe–S clusters in selected enzymes. However, the simple acid–base arguements presented here have a wider application in understanding the results of site-directed mutation experiments in a variety of metalloenzymes.

References

1 W. R. Hagen, in *Bioinorganic Catalysis*, ed. J. Reedijk and E. Bouwman, Marcel Dekker, New York, 2nd edn., 1999, ch 8.

2 R. H. Holm, P. Kennepohl and E. I. Solomon, *Chem. Rev.*, 1996, **96**, 2239 and references therein.
3 G. R. Dukes and R. H. Holm, *J. Am. Chem. Soc.*, 1975, **97**, 528.
4 R. C. Job and T. C. Bruice, *Proc. Natl. Acad. Sci. USA*, 1975, **72**, 2478.
5 B. Shen, L. L. Martin, J. N. Butt, F. A. Armstrong, C. D. Stout, G. M. Jensen, P. J. Stephens, G. N. La Mar, C. M. Gorst and B. K. Burgess, *J. Biol. Chem.*, 1993, **268**, 25928 and references therein.
6 Y. Nicolet, C. Piras, P. Legrand, C. E. Hatchikian and J. C. Fontecilla-Camps, *Structure*, 1999, **7**, 13 and references therein.
7 D. J. Evans, R. A. Henderson and B. E. Smith, in *Bioinorganic Catalysis*, ed. J. Reedijk and E. Bouwman, Marcel Dekker, New York, 2nd edn., 1999, ch. 7.
8 F. Dole, A. Fournel, V. Magro, E. C. Hatchikian, P. Bertrand and B. Guiliarelli, *Biochemistry*, 1997, **36**, 7847 and refs therein.
9 I. Dance, *Chem. Commun.*, 1999, 1655 and refs therein.
10 I. Dance, *Chem. Commun.*, 1998, 523.
11 K. L. C. Gronberg, C. A. Gormal, B. E. Smith and R. A. Henderson, *Chem. Commun.*, 1997, 713.
12 P. J. Stephens, D. R. Jollie and A. Warshel, *Chem. Rev.*, 1996, **96**, 2491 and refs therein.
13 J. R. Dilworth, R. A. Henderson, P. Dahlstrom, T. Nicholson and J. A. Zubieta, *J. Chem. Soc., Dalton Trans.*, 1987, 529.
14 R. E. Palermo, P. P. Power and R. H. Holm, *Inorg. Chem.*, 1982, **21**, 173.
15 G. Christou and C. D. Garner, *J. Chem. Soc., Dalton Trans.*, 1973, 1093.
16 R. A. Henderson, *J. Chem. Soc., Dalton Trans.*, 1982, 917.
17 J. H. Espenson, *Chemical Kinetics and Reaction Mechanisms*, McGraw Hill, New York, 1981, ch. 2.
18 G. M. Sheldrick, *Acta Crystallogr., Sect. A*, 1990, **46**, 467.
19 G. M. Sheldrick, SHELXL, Program for Crystal Structure Refinement, University of Göttingen, Germany, 1993.
20 *International Tables for X-Ray Crystallography*, Kluwer Academic Publishers, Dordrecht, 1992, vol. C, pp. 500, 219 and 193.
21 S. N. Anderson, R. L. Richards and D. L. Hughes, *J. Chem. Soc., Dalton Trans.*, 1986, 245.
22 R. A. Henderson and K. E. Oglieve, *J. Chem. Soc., Dalton Trans.*, 1993, 1467.
23 R. A. Henderson and K. E. Oglieve, *J. Chem. Soc., Dalton Trans.*, 1993, 1473.
24 K. L. C. Gronberg and R. A. Henderson, *J. Chem. Soc., Dalton Trans.*, 1996, 3667.
25 R. A. Henderson and K. E. Oglieve, *J. Chem. Soc., Chem. Commun.*, 1994, 377.
26 R. A. Henderson and K. E. Oglieve, *J. Chem. Soc., Dalton Trans.*, 1998, 1731.
27 R. A. Henderson and K. E. Oglieve, *J. Chem. Soc., Dalton Trans.*, 1999, 3927.
28 V. R. Almeida, C. A. Gormal, K. L. C. Gronberg, R. A. Henderson, K. E. Oglieve and B. E. Smith, *Inorg. Chim. Acta*, 1999, **291**, 212 and refs therein.
29 R. A. Henderson and K. E. Oglieve, *J. Chem. Soc., Chem. Commun.*, 1994, 1961.
30 K. L. C. Gronberg, C. A. Gormal, M. C. Durrant, B. E. Smith and R. A. Henderson, *J. Am. Chem. Soc.*, 1998, **120**, 10613 and refs therein.
31 J. E. Barclay, S. C. Davies, D. J. Evans, D. L. Hughes and S. Longhurst, *Inorg. Chim. Acta*, 1999, **291**, 101.
32 R. A. Henderson, *J. Chem. Soc., Dalton Trans.*, 1999, 119 and refs therein.
33 N. F. Hall and M. R. Sprinkle, *J. Am. Chem. Soc.*, 1932, **54**, 3469.
34 www.cem.msu.edu/~reusch/OrgPage/acidity2.htm.
35 J. F. Coetzee, *Prog. Phys. Org. Chem.*, 1967, **4**, 45 and refs therein.
36 D. Sellmann and J. Sutter, *Acc. Chem. Res.*, 1997, **30**, 460 and refs therein.
37 K. Izutsu, *Acid–Base Dissociation Constants in Dipolar Aprotic Solvents*, Blackwell Scientific, Oxford, 1990.
38 D. M. Smith, B. T. Golding and L. Radom, *J. Am. Chem. Soc.*, 1999, **121**, 9388.
39 H. Beinert, M. C. Kennedy and C. D. Stout, *Chem. Rev.*, 1996, **96**, 2335 and refs therein.
40 J. B. Howard and D. C. Rees, *Chem. Rev.*, 1996, **96**, 2965.
41 C.-H. Kim, W. E. Newton and D. R. Dean, *Biochemistry*, 1995, **34**, 2798.
42 T. H. Rod and J. K. Nørskov, *J. Am. Chem. Soc.*, 2000, **122**, 12751.